JOURNAL OF CATALYSIS 127, 1–8 (1991)

Oxidative Coupling of Methane over Various Metal Oxides Supported on Strontium Carbonate Catalysts

K. AIKA,[1] N. FUJIMOTO, M. KOBAYASHI,† AND E. IWAMATSU

Research Laboratory of Resources Utilization, Tokyo Institute of Technology, 4259 Nagatsuta, Midori-ku, Yokohama 227, Japan

Received December 16, 1989; revised May 29, 1990

The oxidative coupling of methane was studied over unsupported $SrCO_3$ and 20 kinds of (10 mole%) metal oxides (Li, Na, K, Rb, Cs, Mg, Ca, Ba, Al, Pb, La, Y, Zr, V, Cr, Mo, Fe, Co, Ni, and Ag) supported on $SrCO_3$. The prepared catalysts were composed of microparticles of diameters ranging from 0.3 to 100 μm, and were considered to be covered by the oxides added. In general, the oxygen and methane conversions at 1023 or 1073 K increased with an increase of the surface area of the doped catalysts. C_2 selectivity at 1023 K decreased with an increase of methane conversion on the surface area, except for Fe-, Co-, Ni-, Cr-, and Ag-doped catalysts, which produced quite low C_2 selectivity. These results suggest that the catalytic activity or selectivity of catalysts other than Fe, Co, Ni, Cr, and Ag do not differ remarkably from each other at high temperatures (1023 and 1073 K), although there is a trend that Li, Cs, and La oxides are more active and K, Cs, and Y oxides are more selective. Doped oxides were not very effective on $SrCO_3$, but were quite effective on MgO, which can incorporate added cations in the lattice. These results suggest that there is very little interaction between the additives and $SrCO_3$. The XRD study also disclosed that the $SrCO_3$ crystal was not affected by the doping.

INTRODUCTION

The oxidative coupling of methane to give ethane and ethene has interested many researchers as an alternative route for utilizing methane (*1, 2*). Alkaline earth metal oxides (*3, 4*) and lanthanide oxides (*5*) have been widely studied as host oxides. Among alkaline earth metal oxides, MgO and CaO catalysts are often promoted with alkali metal oxides, and have been well studied (*3, 4, 6–10*). SrO and BaO (or $SrCO_3$ and $BaCO_3$) give higher C_2-selectivity, although the activities are lower than those of MgO and CaO (*8, 11*). C_2-yields of MgO and CaO improve when doped with alkali metal oxides (*3, 4, 6, 7, 9, 10*). The doping effects for SrO or BaO have not been reported in detail. The addition of other components to SrO or BaO could improve the activity while maintaining a high level of C_2-selectivity. $SrCO_3$ rather than SrO was selected as a starting material because the surface of carbonate is believed to be partly turned into oxide at 1023 or 1073 K (*11*), and if SrO is used as a starting material, it can react with the quartz glass reactor or can be turned into liquid hydroxides (*8*).

First, we tried to study the effect of additives on $SrCO_3$ in a series of consecutive experiments, based on the previous study of MgO (*7*). Both catalyst morphology and the coupling reaction were studied. No strong promoter effects for the $SrCO_3$ system were observed, which is contrary to the MgO system. Instead, the activities of single component oxides supported on $SrCO_3$ have been compared.

METHODS

The reaction was performed by using a conventional flow reactor (12 mm i.d.) at temperatures from 623 to 1073 K. CH_4, air, and He were charged with flow rates of 1.5

[1] To whom correspondence should be addressed.
† Deceased.

0021-9517/91 $3.00

ml min^{-1} (4.02 mmol h^{-1}), 3.75 ml min^{-1}, and 50 ml min^{-1}, respectively. A ratio of CH_4/O_2 was 2.0 ± 0.1 ($2CH_4 + O_2 = C_2H_4 + 2H_2O$). The selectivity and yield were defined as (2 × moles C_2-compounds produced)/(moles CH_4 reacted) and (2 × moles C_2-compounds produced)/(moles CH_4 in the feed), respectively. Metal nitrates other than V (NH_4VO_3) and Mo ($(NH_4)_6Mo_7O_{24} \cdot 4H_2O$) were added to $SrCO_3$ (Kanto Chemical Co., 99.6%) in water, and the samples then were stirred, dried, pelleted, and weighed. The amount of promoter was expressed as mol% of $SrCO_3$. The pure $SrCO_3$ sample also was made by soaking with water and pelleting (0.8 to 2.4 mm size). A sample of 2 g was treated in a He flow at 773 K for 1 h and at 1073 K for 2 h and then used for the reaction. Use of a full 2 g of sample helped to eliminate the bypassing problem due to the large pellet size (0.8 to 2.4 mm). The surface area was measured after the heat treatment by the BET method, using N_2. SEM pictures were obtained with a Hitachi SEM HFS-2 with an EDX attached (Philips EDAX-707B). XRD spectra were taken with a Rigaku RAD-B system.

RESULTS

Morphological Study by SEM, XRD, and BET

Various doped $SrCO_3$ samples were prepared and evacuated at 1073 K for 2 h. These samples were characterized by the SEM, XRD, and BET methods and also used for the coupling reaction. The SEM pictures of 19 kinds of 10 mol% M–$SrCO_3$ samples (M = metal element), 5 mol% Na^+–$SrCO_3$, 15 mol% Na^+–$SrCO_3$, and $SrCO_3$ are shown in Fig. 1. Alkali metal elements were seen as a pseudoliquid phase covering the $SrCO_3$ particles, especially if the alkali content was high. The other samples seemed to be composed of a coral-like structure. $SrCO_3$ doped with 10 mol% of Li, Na, Rb, Mg, Ba, Y, Zr, and Co were analyzed by XRD. Most of the samples produced nearly the same XRD pattern as $SrCO_3$, which indicates that the additives separated from $SrCO_3$ and are amorphous or form thin crystal coverings. Weak XRD peaks due to additive oxides are seen with Y^{3+}–$SrCO_3$ and Zr^{4+}–$SrCO_3$. Since $SrCO_3$ is insoluble in water, the added soluble nitrates seem to be recrystallized during the drying process and decomposed to oxides during the baking process. $SrCO_3$ seems to act as a support. The particle sizes are quite different from sample to sample. The average particle diameters were measured from TEM pictures and compared with the calculated diameter from BET data-assuming spheres. Both values correspond well, as shown in Fig. 2. All dopants except Zr and Y increased the particle size. Alkali earth metals and especially alkali metals increased the particle diameter, perhaps because the molten salt covering the surface caused the particles to stick together at high temperatures. XRD line broadening can be used to calculate the crystal diameter (*7, 12, 13*). The values obtained with this method are compared with the diameters from SEM pictures in Fig. 3. The crystal diameters (XRD) are smaller than the apparent diameter (SEM) for the various doped samples (shown in Fig. 3). Thus, a model is proposed in which a dopant covers the $SrCO_3$ fine crystals and produces a particle with a diameter larger than that of the crystals. This may be typical of alkali. A model is shown in Fig. 1. EDX analyses show that alkali remains on $SrCO_3$ after the reaction.

It should be noted that XRD line broadening due to the lattice distortion was not observed in this case, which is different from the Na^+–MgO or Rb^+–MgO system (*7*).

Apparent Feature of the Reaction: Temperature Profile and Catalytic Classification

O_2 conversion and CH_4 conversion at 1023 K are shown as a function of the surface area in Figs. 4 and 5. C_2 selectivity and ethene selectivity in C_2 compounds at 1023 K are shown in Figs. 6 and 7. The activities of these catalysts are mostly stable over 100 h.

Alkali metal (Li, Na, K, Rb, Cs) oxides or hydroxides supported on $SrCO_3$ produce

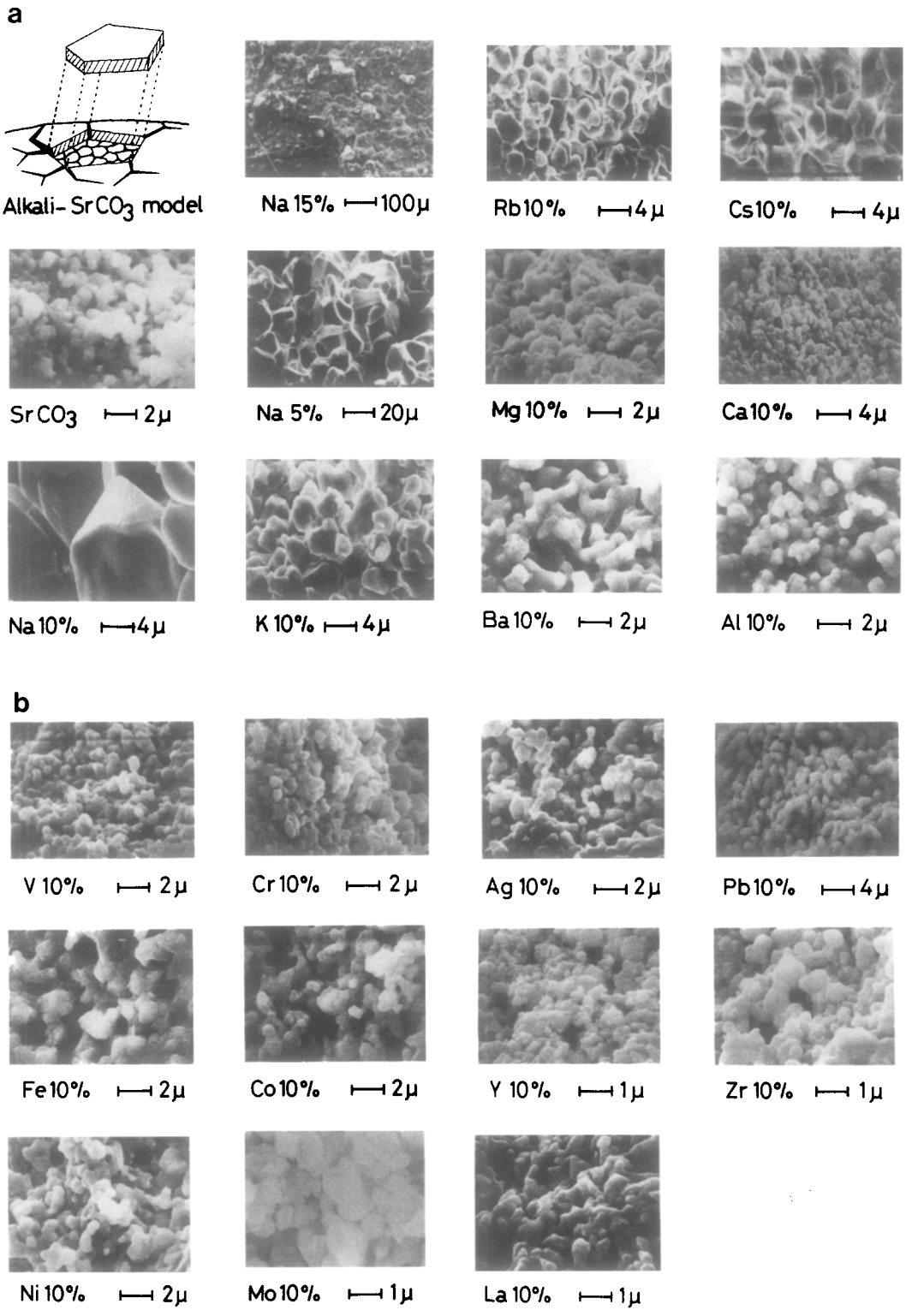

FIG. 1. SEM pictures of $SrCO_3$ catalysts doped with various metal oxides. Doped amounts are expressed as mol% of $SrCO_3$. Samples were evacuated at 1073 K for 2 h.

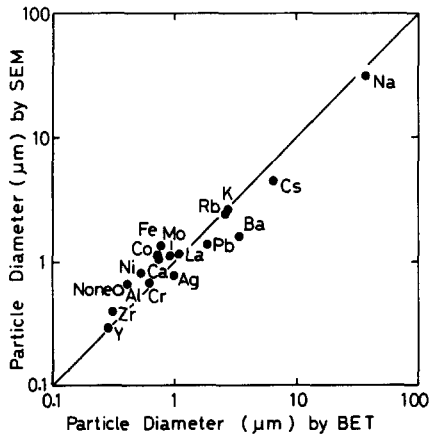

FIG. 2. Comparison of the particle diameters calculated from BET surface area and the average particle diameter in SEM picture. Amounts of doped elements are expressed as 10 mol% of $SrCO_3$. None represent pure $SrCO_3$.

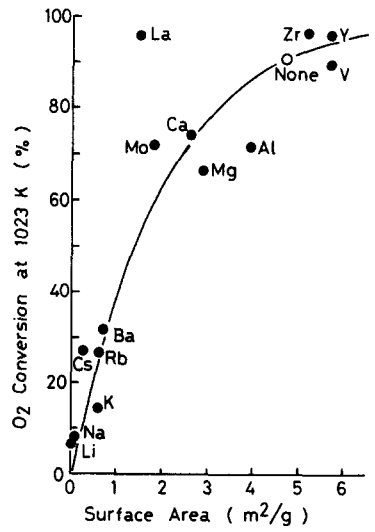

FIG. 4. O_2 conversion of oxidative coupling of methane as a function of specific surface area of 10 mol% doped-$SrCO_3$ catalysts at 1023 K.

low activity, but high selectivity (40 ± 10% at 1023 K and 50 ± 10% at 1073 K). The surface area is low (below 0.6 $m^2\ g^{-1}$). C_2-production is observable above 873 K (using flame ionization detector of GC), while CO_2-production is observable above 973 K (using a thermal conductivity detector of GC).

Alkali earth metal (Mg, Ca, Ba) oxides supported on $SrCO_3$ have higher activities and surface areas than the alkali metal oxides. Both C_2 and CO_2 production are observable above 873 K.

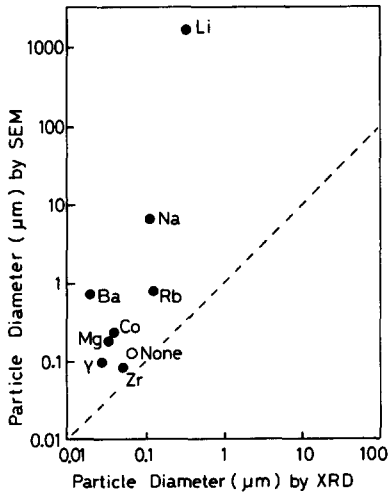

FIG. 3. Comparison of the average particle diameter in SEM picture and that calculated from XRD line broadening. Amounts of doped elements are expressed as 10 mol% of $SrCO_3$. None represent pure $SrCO_3$.

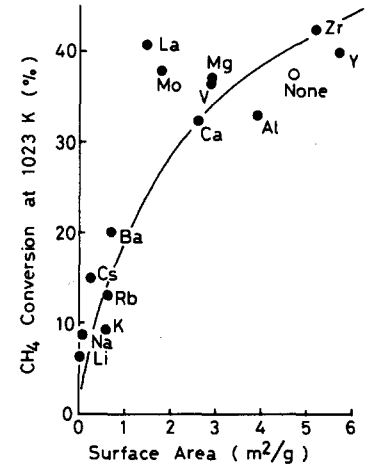

FIG. 5. CH_4 conversion of oxidative coupling of methane as a function of surface area of 10 mol% metal oxide-doped $SrCO_3$ catalysts at 1023 K.

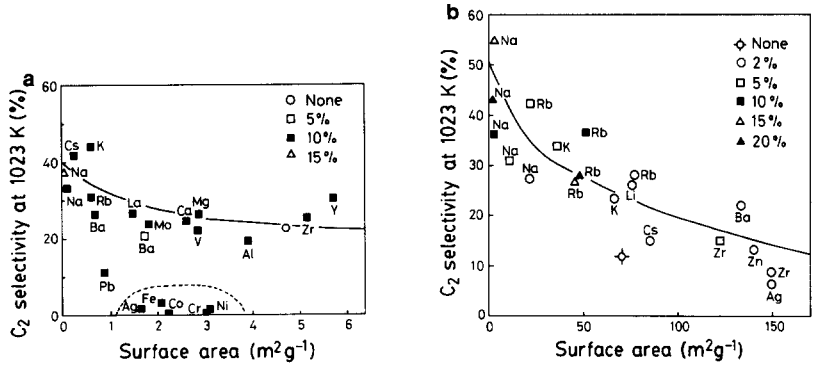

FIG. 6. C_2 selectivity of oxidative coupling of methane as a function of specific surface area at 1023 K over 2 g of metal oxide-doped $SrCO_3$ catalysts (a) and 2 g of metal oxide-doped MgO catalysts (b).

Less active metal (Al, Pb, La, Y, Zr, V, Mo) oxides for oxidation supported on $SrCO_3$ give similar activity and had surface areas comparable to that of $SrCO_3$. CO_2 is produced above 773 K and C_2 production occurs above 873 K. Small amounts of CO were produced on these catalysts above 873 K.

Active metal (Fe, Co, Ni, Cr, Ag) oxides for oxidation supported on $SrCO_3$ have surface areas similar to that of $SrCO_3$ but with higher activities. CO_2-production starts at a lower temperature (773 K) and O_2 conversion exceeds 90% at 873 K. From this temperature upward, C_2-production occurs; however, C_2-selectivity is extremely low.

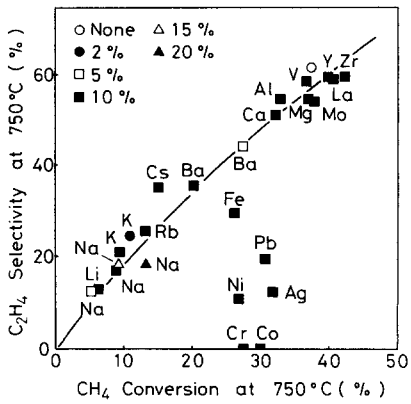

FIG. 7. Ethene selectivity in C_2 compounds by oxidative coupling of methane as a function of CH_4 conversion over metal oxide-doped $SrCO_3$ catalysts at 1023 K.

Reaction Profile at 1023 K

Although the selectivities of the various catalysts differ from each other at lower temperatures, they seem to become closer to each other at higher temperatures (1023, 1073 K), except for the active oxidation elements (Fe, Co, Ni, Cr, Ag). Alkali metal and alkali earth metal oxides, including $SrCO_3$, have some inherent activity. They are poisoned by CO_2, so operation at high temperatures is recommended.

O_2 conversion (x) at 1023 K is plotted as a function of surface area (S) in Fig. 4. The solid line shows the first-order plot with respect to x: $\ln(1 - x) = -0.5\ S$. Most of the catalysts seem to have similar activity; however, Li^+, Cs^+, and La^{3+} appear to be more active than the others. The conversion of methane at 1023 K is also plotted as a function of the surface area in Fig. 5. The same trends can be seen as in the O_2 conversion figures.

C_2-selectivity at 1023 is plotted as a function of the specific surface area in Fig. 6a. C_2-selectivity is generally lower at high surface areas, partly because of the secondary reaction of C_2-compounds to CO_2 and the morphological effect described in the previous papers (*7, 14*). K and Cs give high C_2-

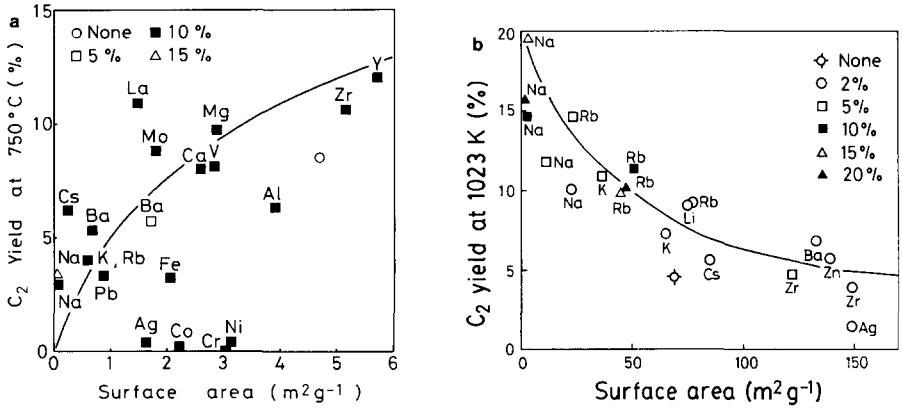

FIG. 8. C_2 yield of oxidative coupling of methane as a function of surface area at 1023 K over 2 g of metal oxide-doped $SrCO_3$ catalysts (a) and 2 g of metal oxide-doped MgO catalysts (b).

selectivities, Y has a relatively high selectivity at a high surface area, and active oxidation catalysts (Ag, Fe, Co, Cr, Ni) give low selectivities. C_2-selectivities on doped MgO catalysts at 1023 K also decrease with an increase in the specific surface area as shown in Fig. 6b (*15*). The results are discussed in the next section.

Ethene selectivity in C_2-compounds at 1023 K is also plotted as a function of CH_4-conversion in Fig. 7. This figure confirms that ethene is a secondary product of the oxidative coupling of methane.

Finally, the C_2-yield at 1023 K is plotted as a function of the surface area (see Fig. 8a). The C_2-yield increases with the surface area. The same plot for doped MgO is shown in Fig. 8b, where the C_2-yield decreases with the surface area (*15*).

DISCUSSION

By being doped with various elements, a surface area can be changed from ca. 0.01 to 6 m^2/g for $SrCO_3$ and from ca. 0.1 to 300 m^2/g for MgO. Reaction profiles of the doped MgO catalyst (2 g) and the doped $SrCO_3$ (2 g) catalysts are compared. CH_4-conversion, C_2-selectivity, and C_2-yield at 1023 K on both catalysts are shown as a function of specific surface area (up to 20 m^2 g^{-1}) in Fig. 9. The solid lines indicate the lines drawn in Figs. 5, 6, and 8, and the dotted lines indicate the expected data. It is clear that the doped MgO is much more active than the doped $SrCO_3$ (see CH_4-conversion in Fig. 9). Two grams of 10 to 20% Na^+–MgO, with an approximate surface area of 1 $m^2 g^{-1}$, gives a CH_4-conversion of about 40% and O_2 conversion of about 95% (*7, 14, 15*). The C_2-selectivity decreases with an increase of the surface area on both catalysts. One of the reasons for the decreased selectivity is that the methyl radical (or methyl peroxide) in the gas phase is oxidized more easily on the increased surface area (*7, 14, 15*). Since the C_2-yield is equal to "CH_4-conversion × C_2-selectivity," it increases with the surface area for the small surface area (0 to 5 $m^2 g^{-1}$ for doped $SrCO_3$ and below 0.3 $m^2 g^{-1}$ for doped MgO; see Ref. (*14*)), whereas it decreases at the high surface area. (It is expected for doped $SrCO_3$ catalyst.)

So, both the activity and selectivity are higher with doped MgO, when compared under the same conditions (surface area, catalyst weight, and temperature). A mechanism including methyl radical as a mutual intermediate both to C_2-compounds and to CO_2 has been proposed to explain these dif-

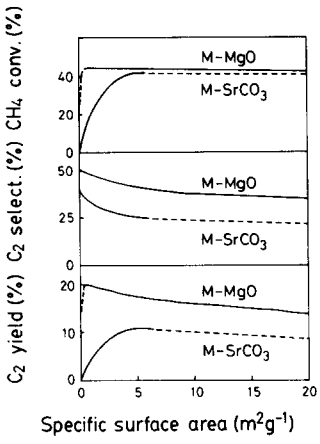

FIG. 9. Comparison of the reaction data over 2 g of metal oxide-doped MgO and 2 g of metal oxide-doped $SrCO_3$ catalysts at 1023 K.

ferences (*7*, *14*, *16*). The steady-state treatment of reactions (1) to (4) gives C_2/C_1 selectivity (R_2/R_1) as shown in Eq. (5) (*14*).

$$O_2 + \text{site} \xrightarrow{2k_1} [\text{oxygen}] \quad (1)$$

$$CH_4 + [\text{oxygen}] \xrightarrow{k_2} \cdot CH_3 + OH(a) + \text{site} \quad (2)$$

$$\cdot CH_3 + xO \xrightarrow{k_3} CO, CO_2 \quad (3)$$

$$2 \cdot CH_3 \xrightarrow{k_4} C_2H_6 \quad (4)$$

$$\frac{R_2}{R_1} = \frac{1}{4}\left(\left(1 + \frac{8k_1k_2k_4P_{O_2}P_{CH_4}}{k_3^2P_{O_2}^{\nu}(k_1P_{O_2} + k_2P_{CH_4})}\right)^{0.5} - 1\right) \quad (5)$$

If the activity is high (in k_1 and k_2), the R_2/R_1 value is high in Eq. (5). The rate of C_2-production is proportional to the second order of methyl radical concentration, while that of C_1 production is proportional to the first order. That is why the active catalyst (doped MgO) produces high C_2-selectivity as is shown in the middle frame of Fig. 9.

Doping of MgO caused both surface area decrease and structural changes (lattice distortion), both of which are thought to increase C_2-yield (*7*). MgO is believed to exchange cations with doped metal ions which distorts the MgO lattice. The effects of Na^+ and Rb^+ ions on MgO have been studied (*7*). Doping of $SrCO_3$ caused the surface area to decrease while no structural change occurred (XRD line broadening is normal). SEM observations also suggest that the dopant is situated on a separated phase of the $SrCO_3$. The added compound is thought to be mounted on the $SrCO_3$ surface, but to have few interactions with $SrCO_3$, due to the large ionic radius of Sr^{2+} and insolubility of $SrCO_3$ in water. MgO may be activated by doping, while $SrCO_3$ is just support material for the dopant. One of the models for alkali-doped $SrCO_3$ is shown in Fig. 1. Alkali–MgO shows a synergic effect (*3*, *7*, *8*), and alkali–$SrCO_3$ does not.

Since the dopant may cover the outer surface, it is considered to be a catalyst. If this is true, it is surprising that the alkali metal oxides, alkali earth metal oxides, and oxides of La, Mo, V, Zr, and Y have similar reactivity and C_2-selectivity at 1023 to 1073 K, although it is clear that La, Li, and Cs have somewhat higher activities (Figs. 4, 5, and 8). The first-order rate constants of all the other elements differ very little. It is interesting to note that the activities of complete oxidation of ethene do not differ markedly among V_2O_5, Cr_2O_3, BaO, CaO, and Al_2O_3 (*17*). Carreiro and Baerns have reported that MgO and CaO are about two orders more active than BaO or SrO, although they are difficult to compare since O_2 conversion is near 100% (*8*). Our results show that Mg, Ca, Ba, and Sr have very similar rate constants. The enhancement of the activity of MgO and CaO is significant only when the oxides are doped with alkali metal oxides. It seems necessary to incorporate some cations of an oxide into the host oxides lattice in order to activate the surface or to produce defects on the surface.

$SrCO_3$ acts as a support, and its surface area can be controlled by mixing with a sin-

gle component, which, when applied pure, has a rather low catalytic activity. However, if $SrCO_3$ is covered with the active mixture (for example Na^+–MgO), better catalysts may be produced.

CONCLUSION

It is difficult to evaluate the catalytic activity of the oxidative coupling of methane, because the activity and selectivity depend not only on the reaction conditions but also on catalyst morphology (*7, 14, 16*). Although we could not produce various catalysts with the same surface area, we were able to compare their activity and selectivity under very similar conditions and morphology by using $SrCO_3$ as a support. The activities of effective oxide catalysts thus are expressed by first-order kinetics and surface area data. While doped MgO catalysts have been thought to have synergistic effects, doped $SrCO_3$ catalysts had few synergistic effects, which may be due to the fact that $SrCO_3$ and dopant produce separate phases.

ACKNOWLEDGMENTS

Prof. T. Onishi, Mr. T. Nishiyama, Mr. K. Tanaka, and Mr. J. W. M. H. Geerts are acknowledged for their assistance with the discussion.

REFERENCES

1. Keller, G. E., and Bhasin, M. M., *J. Catal* **73,** 9 (1982).
2. Hinsen, W., and Baerns, M., *Chem. Z.* **107,** 223 (1983); Hinsen, W., Bytyn, W., and Baerns, M., *in* "Proceedings, 8th International Congress on Catalysis, Berlin, 1984," Vol. 3, pp. 581. Dechema, Frankfurt-am Main, 1984.
3. Ito, T., Wang, J.-X., Lin, C.-H., and Lunsford, J. H., *J. Amer. Chem. Soc.* **107,** 5062 (1985).
4. Moriyama, T., Takasaki, N., Iwamatsu, E., and Aika, K., *Chem. Lett.*, 1165 (1986).
5. Otsuka, K., Jinno, K., and Morikawa, A., *Chem. Lett.*, 499 (1985); Otsuka, K., Liu, Q., Hatano, M., and Morikawa, A., *Chem. Lett.*, 467 (1986).
6. Lin, C.-H., Ito, T., Wang, J. X., and Lunsford, J. H., *J. Amer. Chem. Soc.* **109,** 4808 (1987).
7. Iwamatsu, E., Moriyama, T., Takasaki, N., and Aika, K., *J. Catal.* **113,** 25 (1988).
8. Carrerio, J. A. S. P., and Baerns, M., *J. Catal.* **117,** 258 (1989).
9. Carreiro, J. A. S. P., and Baerns, M., *J. Catal.* **117,** 396 (1989).
10. Nishiyama, T., Watanabe, T., and Aika, K., *Catal. Today* **6,** 391 (1990).
11. Aika, K., Moriyama, T., Takasaki, N., and Iwamatsu, E., *J. Chem. Soc. Chem. Commun.*, 1210 (1986).
12. Scherrer, P., *Gottinger Nachrichen* **2,** 98 (1918).
13. Gallezot, P., *in* "Catalysis, Science and Technology" (J. A. Anderson and M. Boudart, Ed.), Vol. 5, pp. 221. Springer-Verlag, Berlin, 1984.
14. Iwamatsu, E., and Aika, K., *J. Catal.* **117,** 416 (1989).
15. Iwamatsu, E., Moriyama, T., Takasaki, N., and Aika, K., *in* "Methane Conversion" (D. M. Bibby *et al.*, Eds.), pp. 373. Elsevier, Amsterdam, 1988.
16. Iwamatsu, E., Moriyama, T., Takasaki, N., and Aika, K., *J. Chem. Soc., Chem. Commun.*, 19 (1987).
17. Seiyama, T., *in* "Metal Oxides and Catalysis," pp. 14. Kodansha-Scientific, Tokyo, 1978.